26 May 2010, 4:45 pm - 6:45 pm

Dynamic Winkler Modulus for Axially Loaded End-Bearing Piles

George M. Anoyatis
University of Patras, Greece

George E. Mylonakis
University of Patras, Greece


Fifth International Conference on
Recent Advances in Geotechnical Earthquake Engineering and Soil Dynamics
and Symposium in Honor of Professor I.M. Idriss
May 24-29, 2010 • San Diego, California

DYNAMIC WINKLER MODULUS FOR AXIALLY LOADED END-BEARING PILES

George M. Anoyatis
Department of Civil Engineering
University of Patras
Rio, Greece, GR-26500

George E. Mylonakis
Department of Civil Engineering
University of Patras
Rio, Greece, GR-26500

ABSTRACT

The problem of dynamic pile-soil interaction and its modeling through the concept of a Dynamic Winkler Foundation are revisited. It is shown that depth-dependent Winkler springs and dashpots, obtained by dividing the complex-valued soil shear tractions and the corresponding displacements along the pile, may faithfully describe pile-soil interaction, contrary to common perception that the Winkler model is always approximate. A theoretical wave model is then derived for analyzing the response of axially loaded end-bearing piles embedded in a homogeneous viscoelastic soil medium. Closed-form solutions are obtained for: (i) the displacement field in the soil and along the pile; (ii) the impedance coefficients (stiffness and damping) at the pile head; (iii) the depth-dependent Winkler moduli along the pile; (iv) the average, depth-independent, Winkler moduli to match the impedance coefficient at the pile head. Results are presented in terms of dimensionless graphs and charts that highlight the salient features of the problem. The predictions of the model compare favorably with established solutions from the literature, while new results are presented.

INTRODUCTION

The problem of dynamic pile-soil interaction has attracted significant research attention over the past few decades. Most studies focus either on numerical solutions of different levels of rigorousness (Blaney et al. [1976], Nogami [1980], Kaynia & Kausel [1982], Sanchez-Salinero [1982], Banerjee & Sen [1987], Davies et al. [1985]), or on experimental aspects (Novak & Sheta [1982], Blaney et al. [1987], Tazoh et al. [1987], El-Marsafawi et al. [1990], Rollins [1998], Boulanger et al. [1999]). On the other hand, analytical solutions based on wave propagation concepts which can provide realistic predictions and shed light on the complex of physics of the problem have been explored to a much lesser degree (Novak [1974], Nogami & Novak [1976], Dobry & Gazetas [1988], Rajapakse [1990], Ji & Pak [1996]).

It is well known that the most versatile way of modeling soil-pile interaction is through a series of Winkler springs, uniformly distributed along the pile axis. Although approximate, Winkler models are widely used in engineering practice both for axially and laterally-loaded piles subjected to static or dynamic loads (Terzaghi [1955], McClelland & Focht [1958], Coyle & Reese [1966], Novak [1974], Randolph & Wroth [1978], Baguelin & Frank [1979], Scott [1981], Mylonakis [2001]). Their popularity stems primarily from their ability to yield realistic prediction of pile response, incorporate variable soil properties with depth and radial distance from the pile, model group effects and require substantially smaller computational effort than computational-based alternatives.

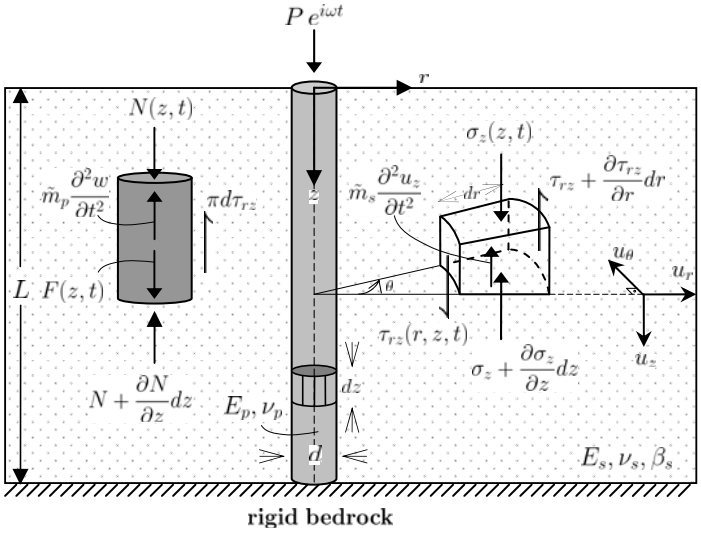

Fig. 1. System considered

Fundamental problem in the implementation of Winkler models lies in the assessment of the modulus of the Winkler springs. Current methods for determining this parameter can be classified into three main groups (Mylonakis [2001]): (A) experimental methods, (B) calibration with rigorous numerical solutions, (C) simplified theoretical models. Notwithstanding the significance of the above methods in geotechnical engineering, they can all be criticized for certain drawbacks. For instance, experimentally-determined *k* values pertain mostly to inelastic conditions and do not properly account for the low-strain stiffness of the soil material (Reese & Wang [1996]). On the other hand, calibrations with rigorous numerical solutions in Group B may encounter numerical difficulties in certain parameter ranges, as for instance, in the case of long compressible piles or high excitation frequencies. Also, these approaches are often limited by the analytical and computational complexities associated with the underlying numerical procedures, which can make then unappealing to geotechnical engineers. Finally, plane-strain models in Group C are either asymptotically unstable, like the Baranov-Novak model which is known to collapse at $\omega = 0$, or require empirical parameters that need to be calibrated with more rigorous methods and do not account for important factors such as the continuity of the medium in the vertical direction and the stiffness contrast between pile and soil (Randolph & Wroth [1978]).

With reference to methods in Group C, it appears that a simple rational model capable of providing improved estimates of Winkler stiffness and damping to be used in engineering application would be desirable. In the framework of linear elastodynamic theory, an approximate yet realistic analytical solution is presented in this paper for an axially loaded end-bearing pile in a homogeneous soil stratum. While maintaining conceptual and analytical simplicity, the proposed model has distinct advantages over other models in Group C, as it accounts for the continuity of the medium in the vertical direction, pile-soil stiffness contrast, pile length to diameter ratio and compressibility of soil material, while being free of empirical constants. Apart from its intrinsic theoretical interest, the proposed model may also be used for the assessment of other related methods.

PROBLEM DEFINITION

The problem considered is depicted in Figure 1: a single solid cylindrical pile embedded in a homogeneous soil medium, subjected to an axial harmonic load of amplitude P and circular frequency ω applied at the pile head. The soil is modeled as a viscoelastic continuum, resisting pile displacements through compression and shearing in the vertical direction. Soil is assumed to be a linear, viscoelastic material, of thickness L, Young's modulus E_s, Poisson's ratio ν_s, mass density ρ_s and linear hysteretic damping β_s, expressed through the complex shear modulus $G_s^* = G_s(1 + 2i\beta_s)$. The pile is described by its length L (same as soil thickness), diameter d, Young's modulus E_p, Poisson's ratio ν_p, mass density ρ_p. Perfect contact (i.e., no gap or slippage) is considered at the pile soil interface. Positive notations for stresses and displacements are provided in Figure 1.

MODEL DEVELOPMENT

With reference to the cylindrical coordinate system of Figure 1, the equilibrium equation of an arbitrary soil element in the vertical direction is

$$\frac{\partial(\tau_{rz}\, r)}{\partial r} + r\,\frac{\partial \sigma_z}{\partial z} + r\,\rho_s\,\frac{\partial^2 u_z}{\partial t^2} = 0 \qquad (1)$$

where τ_{rz} = shear stress on the rz plane, σ_z = normal stress on $r\theta$ plane, ρ_s = soil mass density. $u_z = u_z(r, z, t)$ denotes absolute soil displacement in the vertical direction.
Fundamental to the analysis presented herein is the assumption that the normal stress,σ_z, and the shear stress τ_{rz}, are controlled exclusively by the *vertical* displacement component u_z; the influence of radial displacement, u_r, on these stresses is considered negligibly small.
Based on this physically motivated simplification, the stress-displacement relations for σ_z and τ_{rz} are written

$$\sigma_z \simeq -M_s^*\,\frac{\partial u_z}{\partial z} \qquad (2)$$

$$\tau_{rz} \simeq -G_s^*\,\frac{\partial u_z}{\partial r} \qquad (3)$$

where G_s^* is the complex soil shear modulus and M_s^* a pertinent complex compression modulus to be discussed later on. The negative sign in the right-hand side of the above equations conforms to the positive notation for stresses of Figure 1. It will be shown that this approximation leads to a straightforward uncoupling of the governing Navier equations in the $r$and z directions, unlike the case of the classical elastodynamic equations (Eringen [1962]).

Equations (2) and (3) were apparently first employed by Nogami & Novak [1976] for the analysis of the dynamic pile-soil interaction problem. In that work, however, the radial displacement of the medium was assumed to be zero. In the present study, the assumption would be less restrictive: u_r has negligible influence on σ_z and τ_{rz}, but is not zero. Additional developments over earlier efforts are discussed in the ensuing.
Considering forced harmonic oscillations of the type $u_z(r, z, t) = u_z(r, z, \omega)\, exp(i\omega t)$, the equation of motion is expressed in the Fourier form

$$\frac{\partial^2 u_z}{\partial r^2} + \frac{1}{r}\,\frac{\partial u_z}{\partial r} + \eta_s^2\,\frac{\partial^2 u_z}{\partial z^2} + \left(\frac{\omega}{V_s^*}\right)^2 u_z = 0 \qquad (4)$$

where ω is the cyclic oscillation frequency and η_s^2 a dimensionless parameter which stands for the ratio of the

complex compression modulus to the shear modulus of the soil material

$$\eta_s^2 \;=\; \frac{M_s^*}{G_s^*} \tag{5}$$

As will be demonstrated later in this article, η_s depends solely on Poisson's ratio ν_s. Note that if the variation with depth of the vertical normal stress $\partial\sigma_z/\partial z$ is neglected, equation (4) simplifies to

$$\frac{\partial^2 u_z}{\partial r^2} \;+\; \frac{1}{r}\,\frac{\partial u_z}{\partial r} \;+\; \left(\frac{\omega}{V_s^*}\right)^2 u_z \;=\; 0 \tag{6}$$

which expresses the cylindrical wave equation of the dynamic plane strain model (Baranov [1967], Novak [1974], Novak et al. [1978]). Setting $\omega = 0$ to the above equation, yields the conventional static plane-strain model of Randolph & Wroth [1978] and Baguelin & Frank [1979]. Note that neither equation (4) nor equation (6) exhibit the spurious logarithmic behavior of the static plane strain model, thereby, no empirical corrections need to be employed in the present solution.

Introducing separation of variables, equation (4) yields the general solution

$$u_z = (A\,\sin az + B\,\cos az)\,[C\,I_0(q\,r) + D\,K_0(q\,r)] \tag{7}$$

where $I_0()$, $K_0()$ denote the modified Bessel functions of zero order and the first and second kind, respectively, and a is a real positive variable. A, B, C and D are integration constants to be determined from the boundary conditions. Variable q is connected to a through the frequency-dependent relation

$$q \;=\; \sqrt{(a\,\eta_s)^2 \;-\; \left(\frac{\omega}{V_s^*}\right)^2} \tag{8}$$

To ensure bounded response at large radial distances from the pile and satisfy the boundary condition of zero normal tractions at the soil surface, constants A and C in equation (7) must vanish. Accordingly, the solution simplifies to

$$u_z(r,z) \;=\; B\,K_0(q\,r)\,\cos az \tag{9}$$

in which constant D has been embodied into constant B. Note that for the particular case $q = a\,\eta_s$ (corresponding to $\omega = 0$), the above expression dully reduces to the static solution of Mylonakis [2001].

For a pile of finite length, one must consider the additional condition of vanishing soil and pile displacement at the base of the soil layer. Imposing this requirement on equation (9) yields the discrete values

$$a \;=\; a_m \;=\; \frac{\pi}{2\,L}\,(2m+1), \qquad m = 0,1,2,.. \tag{10}$$

which correspond to the solution of the eigenvalue problem $\cos aL = 0$.

The dynamic response of the soil medium is obtained in form of infinite trigonometric-Bessel series

$$u_z(r,z,\omega) \;=\; \sum_{m=0}^{\infty} B_m\,K_0(q_m\,r)\,\cos a_m z \tag{11}$$

$$\tau_{rz}(r,z,\omega) \;=\; G_s^* \sum_{m=0}^{\infty} B_m\,q_m\,K_1(q_m\,r)\,\cos a_m z \tag{12}$$

The corresponding equilibrium equation for the pile is:

$$\frac{\partial^2 w}{\partial r^2} + \frac{1}{r}\,\frac{\partial w}{\partial r} + \eta_p^2\,\frac{\partial^2 w}{\partial z^2} + \left(\frac{\omega}{V_{sp}^*}\right)^2 w = -\frac{F(z)}{G_p\,A_p} \tag{13}$$

in which $w = w(r,z,\omega)$ is the total vertical displacement of the pile and $V_{sp}^* = V_{sp}\,\sqrt{1+2i\beta_p}$ the complex shear wave propagation velocity in the pile material. Constant η_p is defined as in equation (5), but refers to the pile instead of the soil medium. $F(z)$ stands for external body forces distributed along the pile axis. These can be determined by resolving the force P acting at the pile head into equivalent distributed loads along the pile in the form of Cosine components

$$F(z) \;=\; \sum_{m=0}^{\infty} \frac{2\,P}{L}\,\cos a_m z \tag{14}$$

Introducing separation of variables and accounting for the boundary conditions of zero normal tractions at the soil surface ($z = 0$) and bounded displacements at the pile centerline ($r = 0$), the above differential equation admits the solution

$$w(r,z,\omega) = \sum_{m=0}^{\infty} \left[C_m\,I_0(q_{pm}\,r) \;+\; \frac{2\,P}{G_p\,A_p\,L\,q_{pm}^2}\right]\,\cos a_m z \tag{15}$$

and

$$\tau_{rz}^{(pile)}(r,z,\omega) = -G_p \sum_{m=0}^{\infty} C_m\,q_{pm}\,I_1(q_{pm}\,r)\,\cos a_m z \tag{16}$$

where C_m is an integration constant to be determined from the boundary conditions. In full analogy with the analysis of the soil material, q_{pm} is connected to a_m through the expression

$$q_{pm} = \sqrt{(a_m\,\eta_p)^2 - \left(\frac{\omega}{V_{sp}^*}\right)^2} \tag{17}$$

Imposing the continuity conditions of stresses and displacements at the pile soil interface, constants B_m and C_m can be readily determined. This yields the final solution for pile displacement

$$w(r,z,\omega) = \frac{2\,P}{G_p\,\pi\,L}$$

$$\sum_{m=0}^{\infty} \frac{1}{s_{p_m}^2} \left[1 - \frac{I_0(q_{p_m}\,r)}{I_0(s_{p_m})}\,\frac{X_{2m}\,K_1(s_m)}{K_0(s_m)X_{1m} + X_{2m}K_1(s_m)}\right] \cos a_m z \tag{18}$$

which is valid in the region $0 \le r \le d/2$. In the above equation,

$$X_{1m} \;=\; s_{pm}^2 \tag{19}$$

$$X_{2m} \;=\; \frac{G_s^*}{G_p}\,\frac{I_0(s_{pm})}{I_1(s_{pm})}\,s_m\,s_{pm} \tag{20}$$

with $s_m = q_m\,d/2$, $s_{pm} = q_{pm}\,d/2$ being dimensionless complex parameters.

It is noted in passing that the classical strength-of-materials solution based on the assumption that plane cross sections remaining plane in the pile, is obtained from equation (18) by setting $r = d/2$ and

$$X_{1m} \;=\; a_m^2 \;-\; \frac{\omega^2\,\tilde{m}_p}{E_p^*\,A_p} \tag{21}$$

$$X_{2m} \;=\; \frac{2\,\pi\,s_m\,G_s^*}{E_p^*\,A_p} \tag{22}$$

where $\tilde{m}_p\,(=\rho_p\,A_p)$ is the pile mass per unit length (Anoyatis [2009]). In the ensuing, the Fourier series have been evaluated, with excellent accuracy, using 1000 terms.

Determination of coefficient η

Based on the assumption of vanishing radial displacements, Nogami & Novak [1976] adopted the following form for coefficient η:

$$\eta_s \;=\; \sqrt{\frac{2(1-\nu_s)}{1-2\nu_s}} \tag{23}$$

which expresses the ratio of the constrained modulus to the shear modulus of the soil material. Evidently the above equation exhibits a high sensitivity to Poisson's ratio (recall that η tends to infinity as ν approaches 0.5) which is not observed in rigorous numerical solutions of such problems (Rajapakse [1990], Kaynia & Kausel [1982], Syngros [2004]). To alleviate this drawback, alternative assumptions need to be adopted.

For instance, assuming the horizontal stresses σ_r and σ_θ to be zero yields the pair of equations

$$\eta_s \;=\; \sqrt{2(1+\nu_s)}, \qquad \eta_p \;=\; \sqrt{2(1+\nu_p)} \tag{24}$$

which stand for the ratio of P and S waves in a rod. This is analogous to the assumption used by Veletsos & Younan [1994] for the laterally-loaded problem. A perhaps better choice for the problem at hand is to consider $\sigma_r = 0$ and $\varepsilon_\theta = 0$ which accounts (approximately) for the partial lateral restraint of the soil and the pile material in axisymmetric deformation. In this case,

$$\eta_s \;=\; \sqrt{\frac{2}{1-\nu_s}}, \qquad \eta_p \;=\; \sqrt{\frac{2}{1-\nu_p}} \tag{25}$$

It has been shown (Mylonakis [2001], Anoyatis [2009]) that the predictions of equations (24) and (25) remain close over the entire range of ν values and provide acceptable engineering estimates of vertical pile and soil response under both static and dynamic conditions. Unless specifically otherwise specified, the numerical results presented below are based on equations (25) for the soil and (24) for the pile, using $\nu_s = 0.4$ and $\nu_p = 0.25$.

MODEL VALIDATION

Table 1 compares results for static pile head stiffness for end-bearing piles obtained with the proposed model and from established solutions in the literature. The results are presented

Table 1. Comparison of static pile head stiffness for an end-bearing pile in a homogeneous soil stratum over rigid rock

L/d	E_p/E_s	Normalized static pile stiffness $K_{st}/E_s\,d$				
		Winkler*	Poulos & Davis	Kaynia & Kausel (K)	Proposed model (P)	Difference $\frac{(P)-(K)}{(K)}$: %
10	100	9.78	12.62	10.84	11.18	3.14
	500	41.27	45.17	42.40	42.79	0.92
	1000	80.55	87.74	81.20	82.08	1.08
20	100	7.33	9.07	7.96	8.43	5.9
	500	23.53	26.41	24.28	24.83	2.26
	1000	43.24	46.59	44.00	44.58	1.32
30	100	6.98	8.86	7.28	7.80	7.14
	500	18.66	20.55	19.00	19.62	3.26
	1000	31.99	34.09	32.28	32.99	2.20
40	100	6.92	9.10	7.00	7.57	8.14
	500	16.83	19.91	16.72	17.42	4.19
	1000	27.13	28.34	26.96	27.74	2.89
50	100	6.91	8.67	6.88	7.45	8.28
	500	16.06	18.52	15.56	16.33	4.95
	1000	24.72	28.48	24.12	24.93	3.36

* Winkler solution employs a spring modulus $k = 1.7G_s$

in terms of the normalized static pile head stiffness $K_{st}/E_s\,d$ (Table 1). The performance of the model is satisfactory with maximum deviations over the rigorous solution not exceeding 9%.

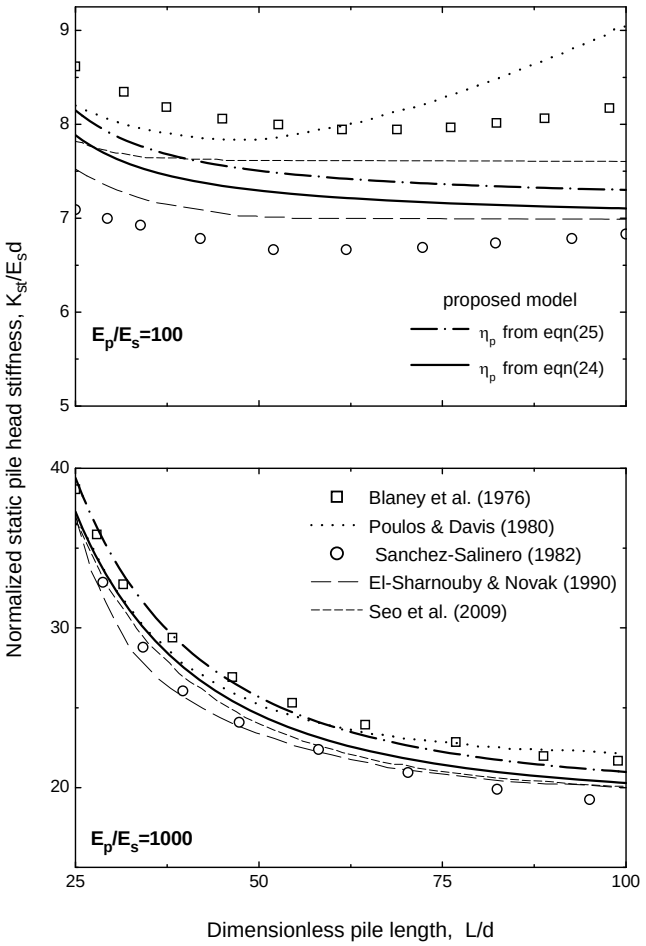

Fig. 2. Static stiffness of end-bearing piles in a homogeneous soil stratum over rigid rock; Comparison of the proposed model with results from published numerical solutions

In Figure 2, results for static pile stiffness obtained from the proposed model are compared to corresponding predictions from finite-element and boundary-element solutions. It can be seen that for small E_p/E_s ratios the numerical results exhibit considerable scattering due to sensitivity to the discretization of the pile. For instance, when a small number of elements is used (Poulos & Davis [1980]), an increase in stiffness with increasing pile length is observed in some of the solutions for $L/d > 50$ - an obviously erroneous trend for an end-bearing pile. El-Sharnouby and Novak [1990] report that a dense discretization (of the order of 50 pile elements or so) is generally needed to remove this anomaly. In contrast, the present solution exhibits a stable behavior and agrees well with the most rigorous results by El-Sharnouby and Novak. Similar good agreement is observed with larger E_p/E_s ratios. Naturally, the longer the pile, the smaller the stiffness at the pile head. This decrease is more pronounced for soft soil.

In dynamic analyses, pile head stiffness can be represented by a complex-valued impedance coefficient K^* which can be cast in the following equivalent forms

$$K^* = \Re(K^*) + i\Im(K^*) = K(1+2i\zeta) \tag{26}$$

where K (real part of K^*) is referred to as storage stiffness and ζ (imaginary part of K^* over twice the real part) as equivalent damping ratio.

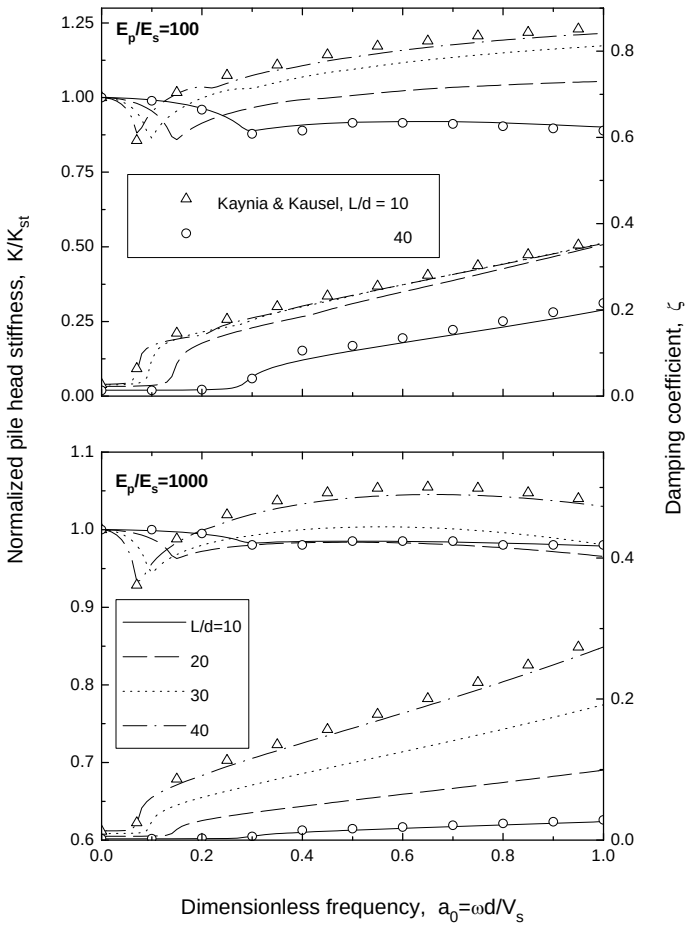

Fig. 3. Comparison of pile head stiffness and damping obtained with the proposed analytical model and from the rigorous solution of Kaynia & Kausel (1982); $\beta_s = 0.05$

A set of comparisons of the predictions of the proposed model against results from the rigorous solution of Kaynia & Kausel is presented in Figure 3 by means of the parameters in equation (26). The results refer to dynamic pile impedance plotted as function of dimensionless excitation frequency. The accord between the proposed model and the numerical solution is very good over the whole range of frequencies examined. This validates the predictive power of the model in the dynamic regime.

The influence of frequency on normalized pile head stiffness becomes more pronounces with soft and long piles. Also, an increase in frequency beyond a threshold value leads to a sudden increase in damping which is attributed to the emergence of propagating waves. This threshold frequency corresponds to the fundamental resonant frequency of the system in compression-extension and is associated with a minimum value in stiffness. It is a simple matter to show that dimensionless resonant frequency $a_{0,cutoff}$ depends solely on soil thickness expressed through the dimensionless slenderness ratio L/d. Higher values of L/d correspond to lower resonant frequencies and vice versa.

In the particular case of $E_p/E_s = 1000$ (Fig. 3b), pile stiffness appears insensitive to frequency as K/K_{st} varies between 1.05 and 0.93, while damping is less than 0.3 over the whole range of frequencies. These results can be understood by recalling that the vertical response of the system is governed mainly by the compliance of the pile rather than that of the soil. For soft piles, the variation of stiffness with frequency is stronger and damping is higher – an anticipated trend for the compliance of the system is controlled to a large extent by the dissipative soil medium. The increase in damping is stronger for long piles and becomes less significant with decreasing pile slenderness ratio.

EVALUATION OF WINKLER MODULUS

The variation with depth of the Winkler modulus k^* can be readily obtained by dividing the vertical soil reaction per unit pile length with the corresponding pile settlement at the pile-soil interface i.e.

$$k^*(z,\omega) = 2\,\pi\,G_s^* \frac{\sum_{m=0}^{\infty} \frac{s_m\ K_1(s_m)\ \cos a_m z}{K_0(s_m)\,X_{1m}\ +\ X_{2m}\,K_1(s_m)}}{\sum_{m=0}^{\infty} \frac{K_0(s_m)\ \cos a_m z}{K_0(s_m)\,X_{1m}\ +\ X_{2m}\,K_1(s_m)}} \tag{27}$$

where the dimensionless parameters X_{1m} and X_{2m} are given by equations (19) and (20). Complex-valued Winkler moduli can be expressed, as before, in the typical form $k^* = k(1+2i\beta)$, k being the dynamic stiffness per unit pile length and β the corresponding damping coefficient. Note that the latter parameter encompasses both material (β_s) and radiation (β_r) damping (i.e., $\beta = \beta_s + \beta_r$).

It is of interest to investigate how load transfer varies along the pile length. For that purpose, normalized pile displacement and soil reaction at the pile-soil interface are plotted against normalized depth in Figures 4 and 5, respectively. In these plots, pile displacement is evaluated at the periphery of the pile i.e. $w_0 = w(d/2, 0)$. It is observed that higher values of pile slenderness generally lead to faster attenuation of pile displacement and soil reaction with depth. In other words, for a given dimensionless depth z/L, displacement and soil

reaction decrease as L/d ratio increases. The trend is more pronounced for soft piles ($E_p/E_s = 100$). For short piles ($L/d = 10$), displacements tend to attenuate linearly with depth indicating a column-like behavior. On the other hand, for long piles linearity is lost and displacements die out exponentially. In particular, for very long piles ($L/d = 100$), considerable drop in tractions and displacements are observed near the pile top and remain significant up to the mid-length of the pile. On the other hand, for $L/d = 10$ the whole pile length contributes equally to attenuation of displacement and side friction.

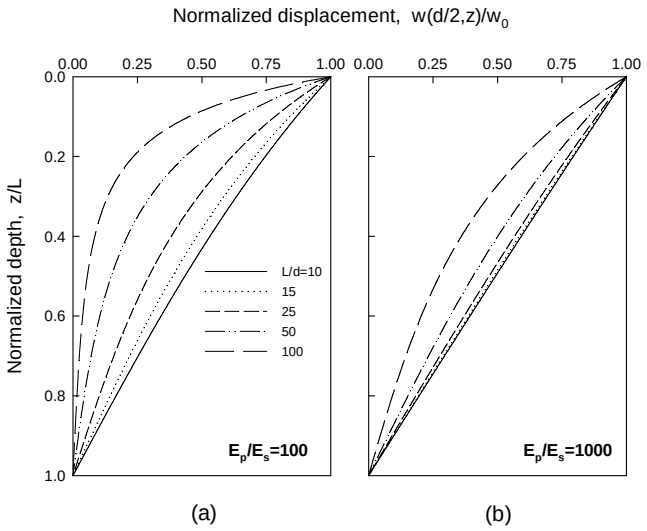

Fig. 4. Variation with depth of pile displacement for an end-bearing pile in a homogeneous soil layer over rigid rock

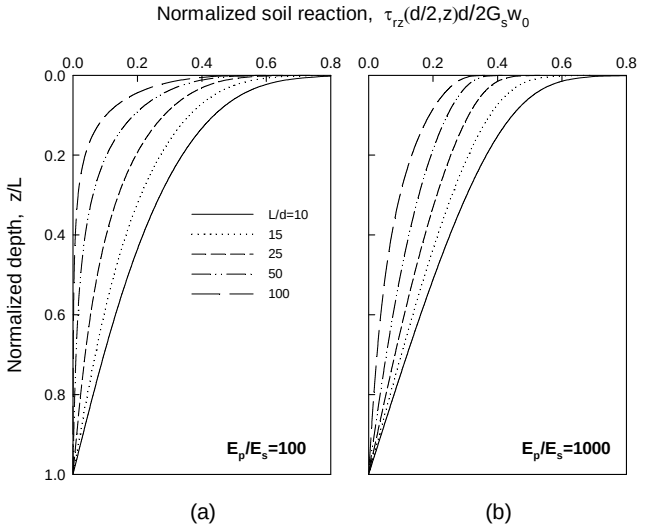

Fig. 5. Variation with depth of soil reaction for an end-bearing pile in a homogeneous soil layer over rigid rock

With reference to static soil reactions, peak values always develop at the pile top and decrease monotonically with depth to become zero at the pile tip (Figure 5). Note that at $z = 0$ a boundary layer ("edge layer") phenomenon develops. This can be understood given that soil reaction at the pile head has to be zero and maximum at the same time (since pile head load has to be resisted at maximum rate whereas shear traction is zero at the soil surface). Evidently, soil reaction has to jump from zero to a local maximum over a very short length generating the aforementioned effect (Syngros [2004]).

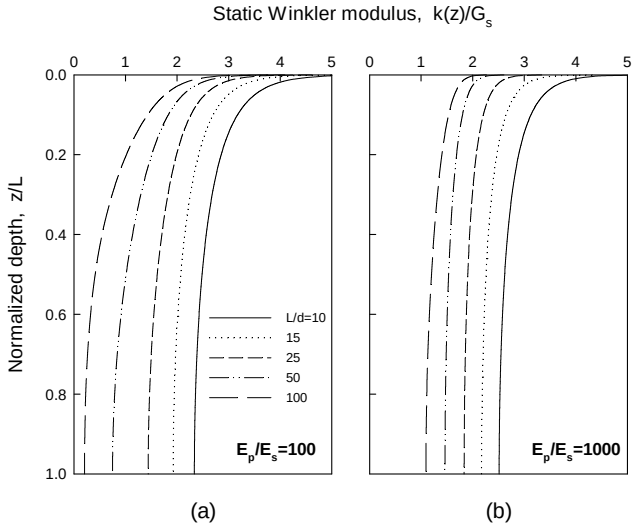

Fig. 6. Variation with depth of static Winkler modulus for an end-bearing pile in a homogeneous soil layer over rigid rock

In Figure 6, the behavior of static Winkler modulus with depth is examined for five different pile configurations. A decreasing trend is observed in all curves. It is observed that in a short pile, $k(z)$ is always larger than the corresponding factor in a more slender pile of same E_p/E_s ratio. Also, the effect of pile-soil stiffness contrast on $k(z)$ is stronger in long piles; for $L/d = 100$ and $E_p/E_s = 100$, $k(z)$ varies between 0.2 and $2.8G_s$; for same L/d and $E_p/E_s = 1000$ $k(z)$ is between 1.1 and $2G_s$. On the other hand, for $L/d = 10$, $k(z)$ is practically independent of stiffness ratio, varying between $2.4 - 4.6G_s$ and $2.5 - 4.2G_s$, for the two stiffness contrasts, respectively. For soft piles, $k(z)$ varies between 0.2 and $5G_s$, whereas for stiff piles the range is restricted to $1.2 - 4.5G_s$. With small E_p/E_s ratios, $k(z)$ tends to increase close to the surface, but decreases more rapidly with depth. The singularity observed at $z = 0$ is due to the aforementioned boundary layer effect and is analogous to that encountered in elastic analysis of surface footings (Pak & Ji [1993]).

Figures 7 to 10 present how dynamic pile displacement and soil reaction vary with depth for different frequencies and a fixed slenderness ratio $L/d = 25$. It is observed that displacements tend to attenuate faster with increasing

frequency. This is anticipated given the increasing contribution of pile and soil inertia with frequency which amplifies soil reaction and causes a phase difference between excitation and response (Fig. 8, 9). This effect is naturally less pronounced for stiff piles (Fig. 7b), with pile displacement following more or less the static curve. In addition, the stiff pile exhibits essentially a column behavior with displacement varying almost linearly with depth regardless of frequency.

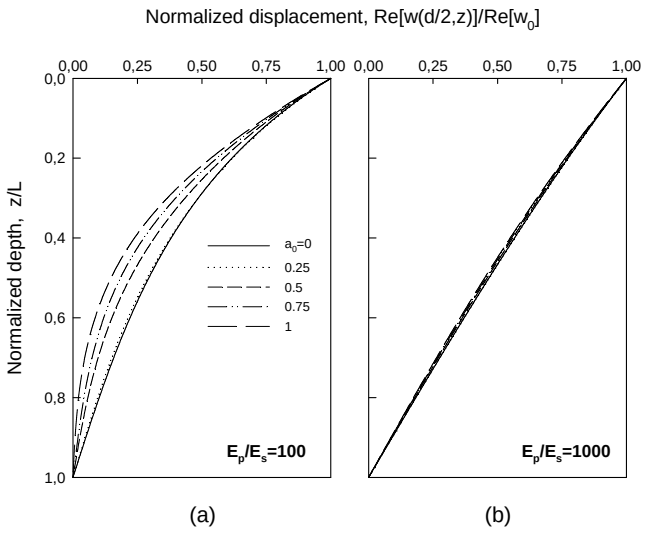

Fig. 7. Variation with depth of normalized dynamic displacement for an end-bearing pile in a homogeneous soil layer over rigid rock, $L/d = 25$, $\beta_s = 0.05$

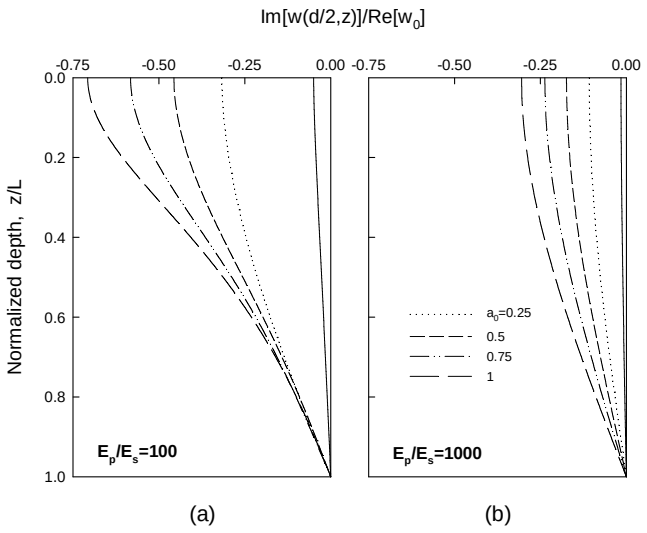

Fig. 8. Variation with depth of normalized dynamic displacement for an end-bearing pile in a homogeneous soil layer over rigid rock; $L/d = 25$, $\beta_s = 0.05$

From Figure 10, it is observed that soil reactions tend to attenuate with depth at a faster rate than pile displacements at the same excitation frequency. The trend is anticipated in light of the Boussinesq solution and becomes more pronounced for soft piles. On the other hand, dynamic tractions appear more sensitive to frequency than displacements, exhibiting increasingly slower attenuation with depth with increasing a_0.

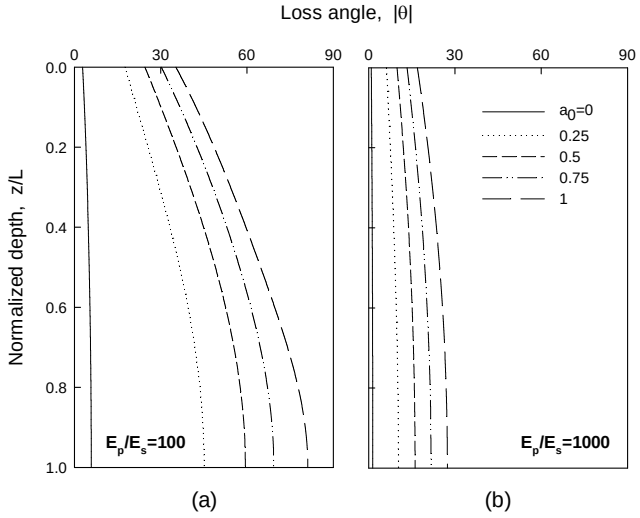

Fig. 9. Variation with depth of amplitude of loss angle for an end-bearing pile in a homogeneous soil layer over rigid bedrock; $\beta_s = 0.05$, $L/d = 25$

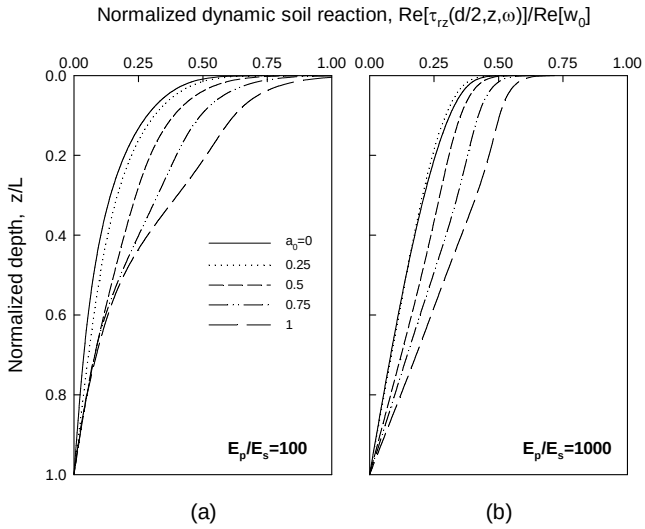

Fig. 10. Variation with depth of normalized dynamic soil reaction for an end-bearing pile in a homogeneous soil layer over rigid rock; $L/d = 25$, $\beta_s = 0.05$

The variation with depth of dynamic spring and dashpots is presented in Figures 11 and 12. As a general trend, dynamic

Winkler moduli and corresponding damping ratios exhibit strong variations with both frequency and depth. At zero frequency ($a_0 = 0$), Winkler modulus naturally decreases monotonically with depth, while damping is almost unaffected by depth, being practically equal to soil material damping β_s. For stiff piles, $k(z)$ varies between 1.6 and $2.8G_s$ over the whole depth and range of frequencies examined. For soft piles the variation is extended to $0.8 - 3.2G_s$. A similar behavior is observed for the damping factor $\beta(z)$ in Figure 12.

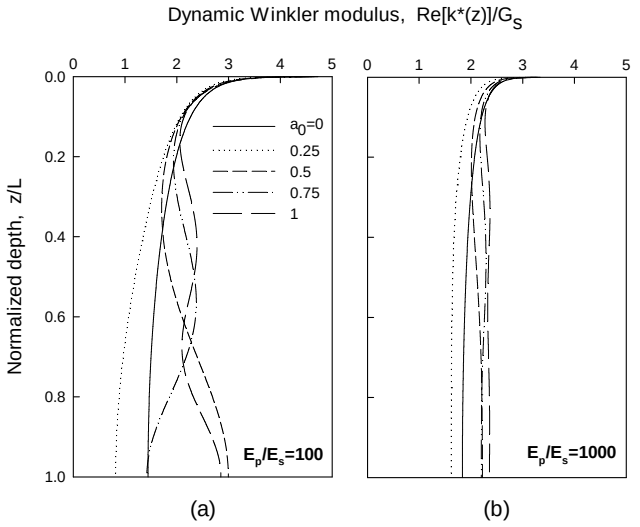

Fig. 11. Variation with depth of dynamic Winkler modulus for an end-bearing pile in a homogeneous soil layer over rigid rock; $L/d = 25$, $\beta_s = 0.05$

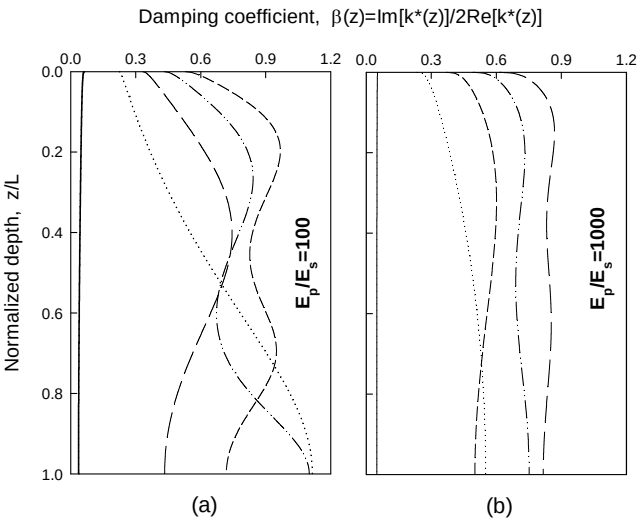

Fig.12. Variation with depth of damping coefficient for an end-bearing pile in a homogeneous soil layer over rigid bedrock; $L/d = 25$, $\beta_s = 0.05$

The oscillatory patterns in the attenuation of dynamic Winkler modulus with depth can be understood by means of the wavelengths of vertically propagating compressional waves in the medium. These are given by the easy-to-derive expressions [Anoyatis 2009]:

$$\lambda_s/d = \frac{2\pi}{a_0}\eta_s \tag{28}$$

$$\lambda_p/d = \frac{2\pi}{a_0}\eta_p \sqrt{\left(\frac{1+\nu_s}{1+\nu_p}\right)\left(\frac{\rho_p}{\rho_s}\right)^{-1}\left(\frac{E_p}{E_s}\right)} \tag{29}$$

λ_s and λ_p referring to wavelengths in the soil and the pile, respectively. These functions are plotted in Figure 13 together with data gleaned from Figure 11. Evidently, observed wavelengths in pile response are associated with waves in the soil medium than waves in the pile. This indicates that pile-soil interaction is mainly governed by wave propagation in the soil than the pile and, thereby, wavelengths are not sensitive to pile-soil stiffness contrast.

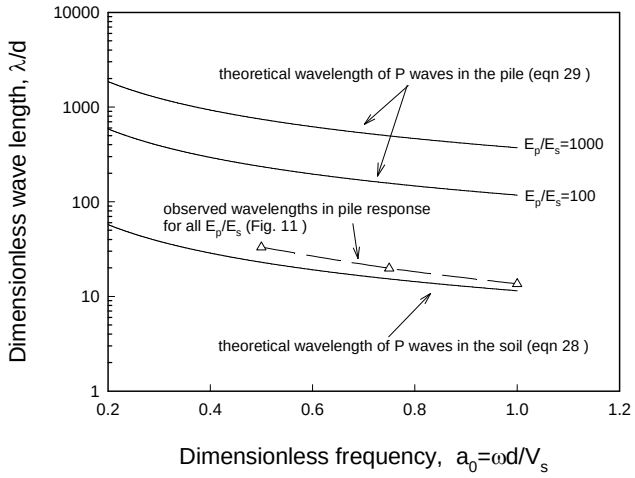

Fig.13. Dependence of P-wavelengths in pile and soil on excitation frequency and pile-soil stiffness contrast

AVERAGE DYNAMIC WINKLER MODULUS

It is well known that dynamic Winkler modulus varies with depth even within a homogeneous soil layer. In practice, however, it is convenient to adopt a constant modulus with depth, to be used in routine engineering calculations. This is usually achieved by equating a key response parameter (e.g., displacement amplitude at the pile head) obtained from the Winkler approach and from a more rigorous solution. Although this simplification naturally introduces some error to the solution, it greatly simplifies the analysis.

Assuming k^* to be constant within a homogeneous soil layer over rigid rock, yields the following solution for the response of an axially-loaded end-bearing pile (Novak [1974])

$$w(z,\omega) = \frac{P}{E_p\, A_p\, \lambda^*}(\cosh \lambda^* z\ \tanh \lambda^* L - \sinh \lambda^* z) \quad (30)$$

where λ is a complex parameter (wavenumber) given by

$$\lambda^* = \sqrt{\frac{\mathbb{k}^* - \omega^2\, \tilde{m}_p}{E_p\, A_p}} \quad (31)$$

Setting the response of the pile head in equations (18) and (30) to be equal, the following implicit solution for $k^*$is obtained.

$$\frac{\tanh L \sqrt{\dfrac{k^* - \omega^2\, \tilde{m}_p}{E_p\, A_p}}}{L \sqrt{\dfrac{k^* - \omega^2\, \tilde{m}_p}{E_p\, A_p}}} =$$

$$(1+\nu_p)\left(\frac{L}{d}\right)^{-2} \sum_{m=0}^{\infty} \frac{K_0(s_m)}{K_0(s_m)\, X_{1m} + X_{2m}\, K_1(s_m)} \quad (32)$$

which can be solved iteratively once the value of the right hand side is determined.

The variation of average static Winkler modulus with pile-soil stiffness is illustrated in Figure 14. It is observed that for pile slenderness ratios less than 50, k is practically independent of pile-soil stiffness contrast. For $L/d > 50$, a slight decrease in k values is observed for soft piles ($E_p/E_s < 1000$). This behavior has been discussed in Mylonakis [2001].

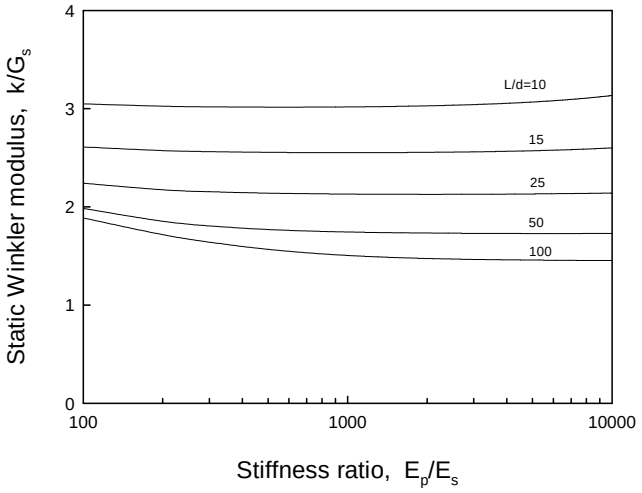

Fig. 14. Average static Winkler modulus for end-bearing piles in a homogeneous soil layer over rigid rock [Mylonakis 2001]

With reference to dynamic Winkler moduli, results obtained from equation (32) are plotted in Figures 15 to 17. The effect of layer thickness on resonant effects and average dynamic Winkler moduli is presented in Figure 15 for pile-soil stiffness contrast $E_p/E_s = 1000$. Resonant effects are associated with the natural frequency of the soil in compression-extension which can be easily obtained from the expression

$$\mathrm{a}_{0,m}^{res} = \frac{\pi}{2}(2m+1)\eta_s \left(\frac{L}{d}\right)^{-1} \quad (33)$$

Evidently, the natural frequency is obtained from the above Equation by setting $m = 0$ and is referred to as cutoff frequency. For frequencies below cutoff, the real part of pile impedance decreases monotonically with increasing frequency approaching zero (for an undamped medium) at $\mathrm{a}_0 = \mathrm{a}_{0,cutoff}$ (Fig. 15a). Over the same frequency range, the imaginary part of the pile impedance is zero (Fig. 15b).

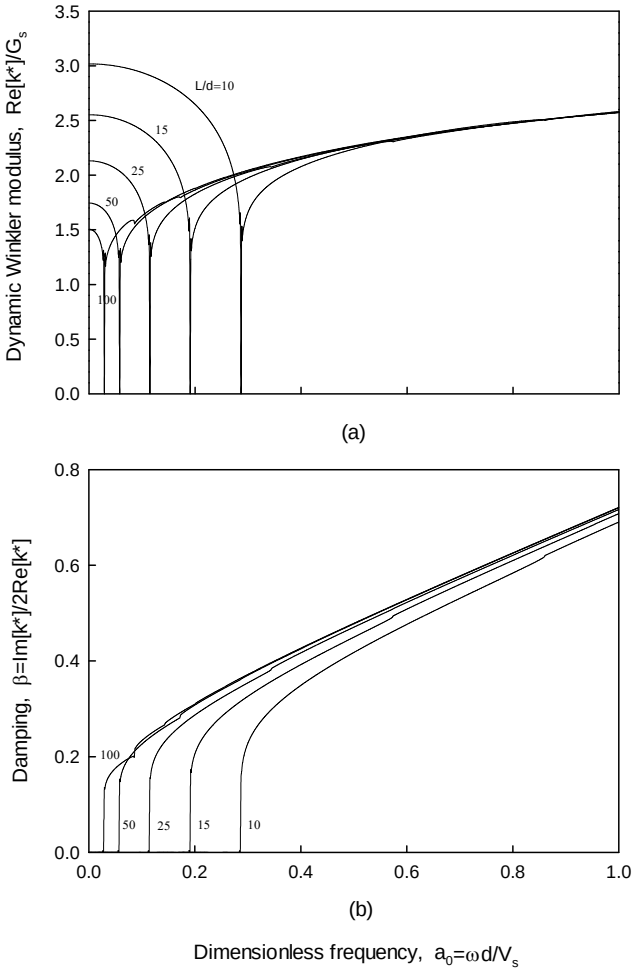

Fig. 15. Variation of average dynamic Winkler impedances with frequency for soil profiles of different thickness; $E_p/E_s = 1000$, $\beta_s = 0$

Beyond cutoff frequency, waves start to propagate in the medium resulting in a sudden emergence of damping. This damping is associated with stress energy dissipation to infinity which is proportional to excitation frequency and, thereby, is referred to as *radiation damping*. Above cutoff, both real and imaginary parts of Winkler modulus increase monotonically with increasing frequency and k becomes less sensitive to the thickness of the soil profile. This indicates that soil thickness is of importance only below cutoff, as all curves converge in the high frequency range.

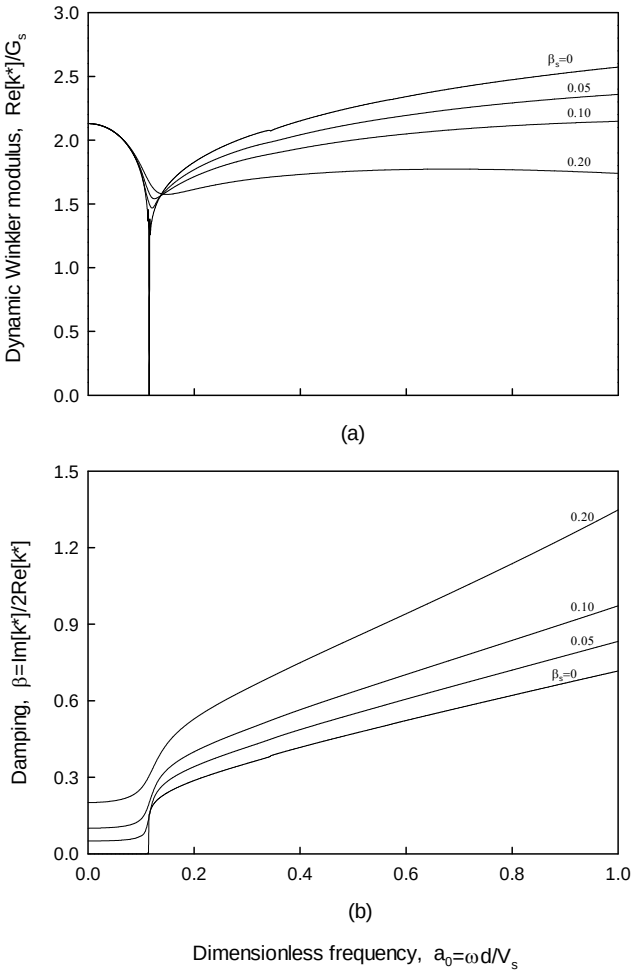

Fig. 16. Effect of soil material damping on average dynamic impedances for end-bearing piles in a homogeneous soil layer over rigid rock; $E_p/E_s = 1000$, $L/d = 25$

The effect of soil material damping on dynamic soil impedance is presented in Figure 16 for pile slenderness ratio $L/d = 25$. For non-zero material damping, stiffness tends to decrease beyond cutoff as compared to an undamped medium, while damping tends to increase. At the cut off frequency, the drop in stiffness is not as dramatic as in the undamped medium. For frequencies below cutoff, damping is practically equal to soil material damping, as zero damping has been considered for the pile. The effect of material damping becomes stronger beyond resonance.

To further explore the role of pile slenderness and pile-soil stiffness ratio on average Winkler moduli, Figure 17 presents results for extreme values of E_p/E_s and L/d. A clear trend is observed: a reduction in soil stiffness (a conservative assumption in the realm of static analysis) leads to an increase in radiation damping, resulting to non-conservative results in the dynamic regime (Syngros [2004]). This behavior is pronounced for slender piles and does not exist for short piles.

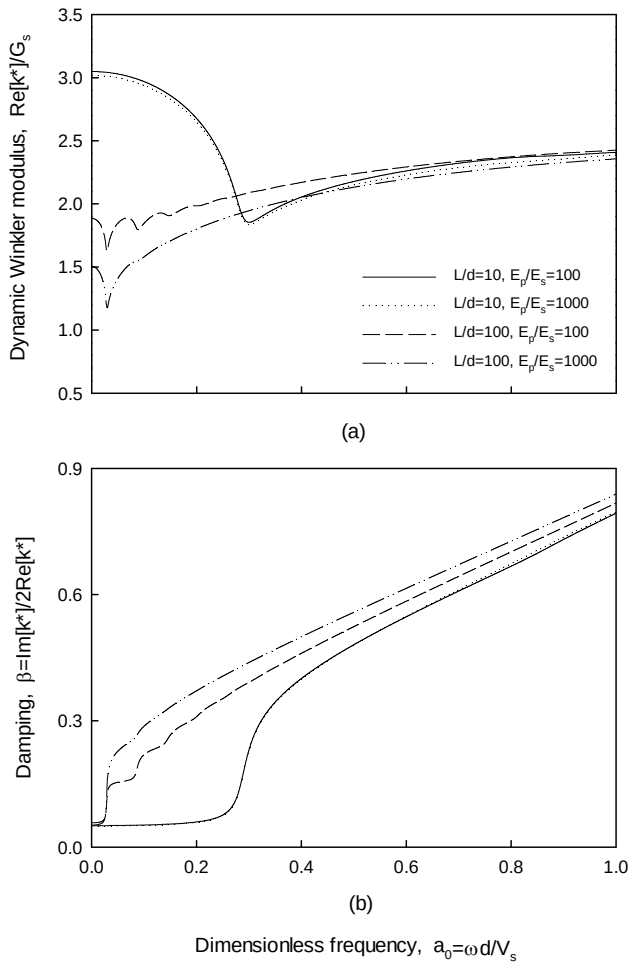

Fig. 17. Effect of pile slenderness and pile-soil stiffness ratio on average dynamic impedance for end-bearing piles in a homogeneous soil layer over rigid rock; $\beta_s = 0.05$

CONCLUSIONS

Dynamic pile-soil interaction was analytically investigated through an approximate elastodynamic model by using the concepts of a continuum and a Winkler support. The proposed model yields solutions for the complex-valued shear tractions along axially-loaded end-bearing piles in a homogeneous

viscoelastic soil stratum. Rigorous numerical results (Kaynia & Kausel, 1982) were employed to validate the predictions of the analytical model.

The main conclusions of the study are:

1. The model has sufficient predictive power and is self standing, as it compares well with rigorous numerical solutions and does not involve empirical constants.
2. Dynamic Winkler modulus, like its static counterpart, is depth-dependent even in homogeneous soil.
3. A boundary layer phenomenon is observed at the pile head, and is attributed to the counteracting requirements for zero and maximum side resistance at pile head. This effect appears to be of limited practical significance.
4. Pile soil interaction is mainly governed by wave propagation in the soil, not on the pile. Thereby wavelengths depend mostly on frequency – not on pile-soil stiffness contrast. However, Winkler moduli depend both on frequency and pile-soil stiffness contrast.
5. Reducing soil stiffness (a conservative assumption in the realm of static analysis) leads to an increase in radiation damping, thereby it may result to non-conservative estimates of dynamic pile response.
6. In the high frequency range, storage stiffness of Winkler springs is independent of pile slenderness. For the pile-soil configurations examined in this study, all impedance curves converge for dimensionless frequencies above approximately 0.5.
7.

As a final remark, it is fair to mention that the proposed model is limited by the assumptions of linearity in soil and the pile material, as well as perfect bonding at the pile-soil interface. Exploring these effects lies beyond the scope of this study.

REFERENCES

Anoyatis, G. [2009]. "Elastodynamic Pile Analysis under Inertial and Kinematic Loading", MSc Thesis, University of Patras.

Baguelin, F. and Frank, R. [1979]. "Theoretical Studies of Piles using the Finite Element Method", In Numerical Methods in offshore piling, pp. 83-91. Institution of Civil Engineers.

Banerjee, P.K. and Sen, R. [1987]. "Dynamic Behavior of Axially and Laterally Loaded Piles and Pile Groups", Dynamic Behavior of Foundations and Buried Structures, Elsevier, New York, pp. 95-113.

Baranov, V. A. [1967]. "On the Calculation of an Embedded Foundation (in Russian), Vorposy Dinamiki i Prognostic", Polytechnical Institute of Riga, Latvia, No. 14, pp. 195-209.

Blaney, G.W., Kausel, E., Roesset, J.M. [1976]. "Dynamic Stiffness of Piles", Proc 2nd Int. Conf, Num. Methods Geomech, Blacksburg, 1001-1012.

Blaney, G.W., Muster, G.L., O'Neil, M.W. [1987]. "Vertical Vibration Test of a Full-scale Pile Group", ASCE Geotech. Special Publication, No. 11, pp. 149-165.

Boulanger, R.W., Curras, C.J., Kutter, B.L., Wilson. D.W.,Abghari, A. [1999]. "Seismic Soil-Pile-Structure Interaction Experiments and Analyses". Journal of Geotechnical and Geoenvironmental Engineering, ASCE 125, No. 9, pp. 750-759.

Coyle, H.M. and Reese, L.C. [1966], "Load Transfer for Axially Loaded Piles in Clay", J. Soil Mech. Found. Div., ASCE 92, No. SM2, pp. 1-26.

Davies, T.G., Sen, R., Banerjee, P.K. [1985]. "Analysis of Laterally Loaded Piles in Soft Clays", J. Geotech. Engng. Vol. 114, No. 1, pp. 21-39.

Dobry, R. and Gazetas, G. [1988]. "Simple Method for Dynamic Stiffness and Damping of Floating Pile Groups", Geotechnique 38, No. 4, pp. 557-574.

El-Marsafawi, H. and Kaynia, A.M., Novak, M. [1990]. "Interaction Factors and the Superposition Method for Pile Group Dynamic Analysis", Geotechnical Research Center Report, GEOT-1-92, The University of Western Ontario.

El-Sharnouby, B. and Novak, M. [1990]. "Stiffness Constants and Interaction Factors for Vertical Response of Pile Groups", Can. Geotech. J. 27, pp. 813-822.

Eringen, A.C. [1962]. "Nonlinear Theory of Continuous Media", MacGraw-Hill.

Kaynia, A. M. and Kausel, E. [1982]. "Dynamic Stiffness and Seismic Response of Pile Groups", Research Report R82-03, Massachussets Inst. of Technology.

McClelland, B. and Focht, J. [1958]. "Soil Modulus for Laterally Loaded Piles", Transactions of the American Society of Civil Engineers, Vol. 123, pp. 1049-1086.

Mylonakis, G. [2001]. "Winkler Modulus for Axially Loaded Piles", Geotechnique 51, No. 5, pp. 455-461.

Nogami, T. and Novak, M. [1976]. "Soil-pile Interaction in Vertical Vibration", Earthquake Engrg & Struct. Dyn. 4, pp. 277-293.

Nogami, T. [1980]. "Dynamic Stiffness and Damping of Pile Groups in Inhomogeneous Soil", Dynamic Response of Pile Foundations (Eds O'Neil, M. and Dobry, R.), ASCE, New York, 1980

Novak, M. [1974]. "Dynamic Stiffness and Damping of Piles", Can. Geotech. J., 11, pp. 574-598.

Novak, M., Nogami, T. and Aboul-Ella, F. [1978]. "Dynamic Soil Reactions for Plane Strain Case", J. Engng Mech. Div., ASCE 104, No. 44, pp. 953-959.
Novak, M., Sheta, M. [1982]. "Vertical Vibrations of Pile Groups", J. Geotech Engng, ASCE 108, pp. 570-590.

Pak, R.Y.S and Ji, F. [1996]. "Scattering of Vertically-Incident P-Waves by an Embedded Pile", Soil Dyn. and Earthquake Engrg, Vol. 15, No. 3, pp. 211-222.

Pak, R.Y.S. and Ji, F. [1993]. "Rational Mechanics of Pile-Soil Interaction", J. Engng. Mech., ASCE 119, No. 4, pp. 813-832.

Poulos, H.G. and Davis, E. [1980]. "Pile Foundation Analysis and Design", Wiley, New York.

Rajapakse, R.K.N.D. [1990]. "Response of an Axially Loaded Elastic Pile in a Gibson Soil", Geotechnique 40, No. , pp. 237-249.

Randolph, M. F. and Wroth, C. P. [1978]. "Analysis of Deformation of Vertically Loaded Piles", J. Geotech. Engng, ASCE, 104, No. 12, pp. 1465-1488.

Rollins, K.M., Peterson, K.T., Weaver, T.J. [1998]. "Lateral Load Behavior of Full-scale Pile Group in Clay", J. Geotech. and Geoenvir. Engng, ASCE 124, No. 6, pp. 468-478.

Sanchez-Salinero, I. [1982]. "Static and Dynamic Stiffness of Single Piles". Geotech Engng Rep. GR82-31. Austin: University of Texas

Scott, R.F. [1981]. "Foundation Analysis", Prentice Hall.

Seo, H., Basu, D., Prezzi, M., Salgado, R. [2009]. "Load-settlement Response of Rectangular and Circular Piles in Multilayered Soil", J. Geotech. and Geoenvir Engng, ASCE 135, No. 3, pp. 420-430.

Syngros, K. [2004]. "Seismic Response of Piles and Pile-Supported Bridge Piers Evaluated through Case Histories", Phd Thesis, City University of New York.

Tajimi, H. [1969]. "Dynamic Analysis of a Structure Embedded in an Elastic Stratum", Proceedings 4th WCEE, Chile.

Tazoh, T., Shimizu, K., Wakahara, T. [1987]. "Seismic Observations and Analysis of Grouped Piles", Dynamic Response of Pile Foundations: experiment, analysis and obsrvartion, Geotechnical Special Publication, ASCE, No. 11.

Terzaghi, K. [1955]. "Evaluation of Coefficients of Subgrade Reaction", Geotechnique, Vol. 5, No. 4, pp. 297-326.

Veletsos, A. S. and Younan, A. H. [1994]. "Dynamic Soil Pressures on Rigid Cylindrical Vaults". Earthquake Engng & Struct. Dyn. 23, pp. 645-669.